A Modified Fluorescent Lamp for Discreet Biometric Surveillance

John J. Cooley
Massachusetts Institute of Technology
MIT Rm. 10-007
Cambridge, MA 02139
Email: jjcooley@mit.edu

Al-Thaddeus Avestruz
Massachusetts Institute of Technology
MIT Rm. 10-017
Cambridge, MA 02139
Email: avestruz@mit.edu

Steven B. Leeb
Massachusetts Institute of Technology
MIT Rm. 10-069
Cambridge, MA 02139
Email: sbleeb@mit.edu

***Abstract*—A standard 48-inch two-bulb fluorescent lamp was modified to be used as a capacitive sensing system. The lamp sensor system demonstrated the ability to detect the presence and motion of human targets at ranges of up to 10 feet between the lamp and the closest edge of the target. Proof of concept was also demonstrated for metal detection by demonstrating the ability to differentiate between a human target and the same human target carrying conducting (metallic) objects. The lamp sensor shows potential for low-cost and widespread discreet security monitoring and biometric surveillance.**

I. Introduction

By making use of the alternating electric fields emitted by a fluorescent lamp under normal operation, the lamp can be used as a capacitive sensor. The lamp sensor demonstrated proof of concept in [1] for detecting the presence and motion of human targets at maximum distances of up to 10 feet below the lamp. The functionality of the lamp sensor is extended from [1] by detecting the presence of metallic objects on the human target. Also, by using multiple electrode pairs spaced differently, instead of only one electrode pair, the capability to scan vertically is explored and the concept of the lamp sensor as a discreet biometric surveillance sensor is demonstrated. In this vertical scanning technique, materials with anomalous dielectric or conductive make-up can be seen as anomalies in the output voltage of the lamp sensor system.

II. Background: Lamp Sensor Concepts and Signal Conditioning

A. Balanced Source for Differential Measurements

In our system, two electrodes measure electric field disturbances below the lamp with a differential measurement from two electrodes. The differential measurement offers several advantages. First, the differential measurement eliminates the dependence on any dc ground reference when measuring the electric fields emitted by the lamp. Second, the differential topology is insensitive to common-mode pickup or interference likely to be present on account of other electric field sources. Third, because the differential measurement is taken from a balanced topology, the differential gain of the front-end amplifier in the signal conditioning circuitry can be very large without saturating, because in the absence of a detection the output is nulled. Small deviations from the nulled output can be amplified greatly.

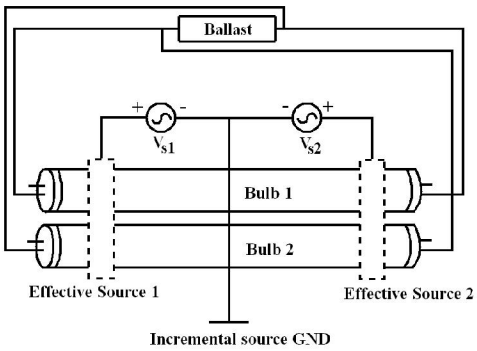

Fig. 1. Reversing the ballast connections to one bulb results in symmetric effective voltage sources referenced to the center of the lamp [2].

The lamp sensor system presented in [1], [2] and here uses a 48-inch, two-bulb lamp. In order to implement a differential and balanced measurement, we modify the ballast connections to the two bulbs so that the source of electric field from the bulbs is symmetric about the center of the lamp. Without modifying the ballast connections, the bulbs are driven in phase (current flowing the same direction in each bulb) and the alternating voltage relative to the center of the bulbs for one side of the lamp is 180° out of phase with the alternating voltage relative to the center of the bulbs for the other side. In that case, the lumped signal source, consisting of the sum of the alternating voltages of the two bulbs, is not symmetric and therefore not ideal for our differential measurement. By reversing the ballast connections to one of the bulbs, the sum of the alternating voltages of the two bulbs is symmetric about the center of the lamp. The sum, however, will be nonzero because the voltage waveform of each bulb is asymmetric about the center of the lamp. A typical length-wise voltage profile of a struck fluorescent bulb can be found in [5]. A diagram of the ballast connections to the two bulbs and the balanced effective signal sources is shown in Figure 1.

The effective strength of the alternating voltage source in the context of the differential measurement between two electrodes is complicated because it depends on the electrode

1-4244-1053-3/07/$25.00 ©2007 IEEE.

configuration (distance between the electrodes and the lamp and distance between the two electrodes), the asymmetric voltage profile of each bulb, and on the geometry of the lamp. Because the absolute strength of the effective voltage source is only necessary for predicting absolute responses, it is not generally measured directly (in [1], [2], nor here), although it can be inferred for each electrode configuration by comparing simulated responses to measured responses as in [2]. The treatment of the electrical signal source as a low-impedance voltage source and not a high-impedance current source is discussed in [2].

B. Capacitive Model

Measuring electric field changes below the lamp in response to a conducting or dielectric target amounts to measuring changes in lumped capacitance values between conducting surfaces. The simplified physical capacitive model of the lamp sensor and target is shown in Figure 2. The physical model consists of the capacitances of interest between conducting surfaces including the lumped signal source and the human target. For simulation, capacitance values are readily obtained using the multipole-expansion finite-element modeling software FastCap [4]. The treatment of all of the capacitances in the system and the simplification to the model shown here can be found in [2].

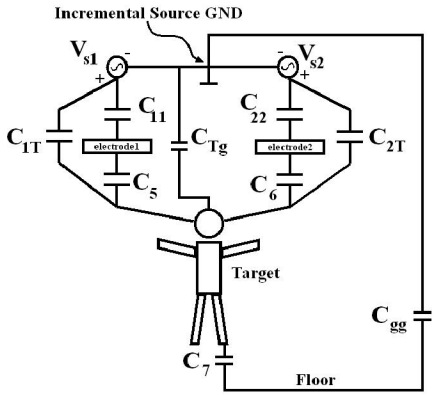

Fig. 2. The lumped element capacitive model consists of capacitances of interest between conducting surfaces and the lumped signal sources in the lamp sensor and target system. The full treatment of all of the capacitances in the real system and the simplification of the full model to the model shown here can be found in [2].

Table I provides a description of the lumped capacitances in the simplified physical model and nominal values obtained from FastCap [4]. Capacitances that vary depending on the position of the human target below the lamp have a range of capacitances that is lower bound by the minimum detectable change in capacitance in the system presented here.

The lumped capacitive model is simplified and redrawn as the capacitive circuit shown in Figure 3. The measured signal is the differential current that passes through the effective low-impedance path from one electrode to the other created by the differential transimpedance amplifier presented in Section II-C.

TABLE I
CAPACITANCE DESCRIPTIONS AND NOMINAL VALUES FOR THE LUMPED CAPACITANCE MODEL [2].

Label	Physical Description	Nominal Value(s)
C_{11}	Left source to left electrode	2 pF
C_{22}	Right source to right electrode	2 pF
C_{1T}	Left source to target	10 fF-1 pF
C_{2T}	Right source to target	10 fF-1 pF
C_5	Left electrode to target	10 fF-1 pF
C_6	Right electrode to target	10 fF-1 pF
C_7	Target to floor	10 pF
C_{gg}	Floor to incremental bulb ground	1 pF
C_{Tg}	Target to incremental bulb ground	1 pF

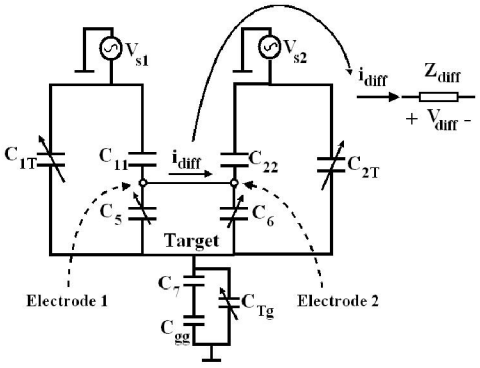

Fig. 3. The lumped element capacitive circuit consisting of the capacitances of interest shows a symmetrical and balanced bridge circuit for nullable differential measurement. The differential signal that will be measured is the differential current i_{diff} and it will be measured as the differential voltage v_{diff} at the output of a differential transimpedance amplifier with differential transimpedance Z_{diff} [2].

C. Signal Conditioning

The capacitive circuit presented in Section II-B is interfaced with signal conditioning circuitry by connecting the electrodes to an analog front-end amplifier with shielded cables. The electrodes are connected directly to the high-impedance inputs of a high-gain op-amp. The result is current-mode detection of the signals in the capacitive circuit of Figure 3. Therefore, the amplifier, after the effective input capacitance from the capacitive circuit, is a transimpedance amplifier. The schematic of the implemented transimpedance amplifier is shown in Figure 4. The JFET op-amps buffer the inputs of the fully-differential op-amp for low input-offset current and low input-referred current noise. Feedback capacitors stabilize the system with a form of lead compensation in order to provide a stable closed-loop response despite the capacitive input elements.

1) Stray Capacitances: One advantage of using current-mode detection (by connecting the electrodes directly to the inputs of the front-end op-amp) is that stray capacitances from the electrodes to incremental ground can be neglected in the output response of the front-end amplifier. The fully-differential circuit consisting of the signal source and front-end amplifier can be separated into two identical half-circuits. The voltage reference for each half-circuit is the voltage about which the two halves of the differential voltages in the fully differential circuit are symmetric. Figure 5, shows the half-

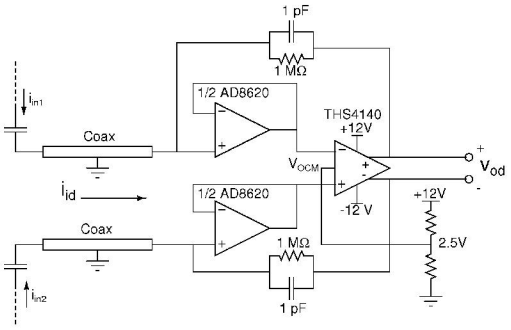

Fig. 4. Schematic of the Low-Noise Analog Front-End Amplifier [2]

circuit in which the ground reference is labeled "differential ground reference." The stray capacitance, C_{stray}, shunts the op-amp input node to the differential ground [2].

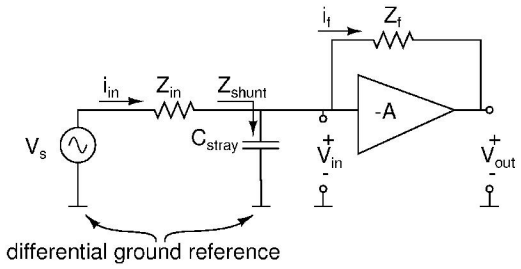

Fig. 5. The fully-differential circuit can be separated into two identical half-circuits. The half-circuit voltages vary with respect to the differential ground reference.

In the closed-loop connection shown in Figure 5, the output voltage, V_{out}, of the half-circuit varies with respect to the differential ground reference. If the differential gain of the op-amp is $A(s)$, the input voltage variation relative to the ground reference is attenuated by $|A(j\omega)|$ from the output voltage. Because $|A(j\omega)|$ is large by design, the input voltage of the op-amp, V_{in}, varies very little relative to differential ground reference. Since the small variation in V_{in} appears across C_{stray}, the stray capacitance does not shunt much current from the input current, i_{in}. Therefore, the stray capacitance can be neglected. C_{stray} is "bootstrapped" because the voltage variation across it is small. The effective impedance, Z_{eff} of the bootstrapped stray capacitance is $Z_{shunt}/|A(j\omega)|$ [2], [3].

As an example, the relatively large (30 pF) shield capacitance of the coaxial cables connecting the electrodes to the amplifier can be conveniently neglected. The shield capacitances are connected to board ground which differs from the differential ground reference. However, the impedance from the input node to the differential ground reference through the shield capacitances must be at least as large as the impedance from the input node to board ground [2].

2) Synchronous Detection: The signal conditioning circuitry uses synchronous detection to isolate the effect of the symmetric alternating signal source on the capacitive system from other stray signals that differ either in frequency or in phase. In the synchronous detection scheme, the carrier signal is the alternating voltage source signal and the baseband signal results from the changes in the effective input capacitance due to the presence or movement of the target below the lamp. A modulated carrier signal or an up-modulated baseband signal results from the carrier signal driving current through the changing effective input capacitance. The signal is down-modulated back to the baseband after amplification. This is accomplished by multiplication with another copy of the carrier signal. A simplified block diagram of the synchronous detection system is shown in Figure 6.

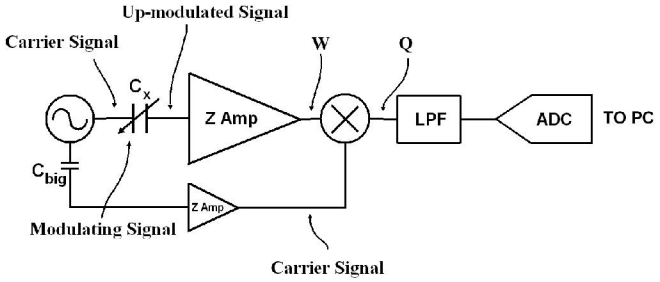

Fig. 6. A simplified block diagram of the synchronous detection system detects changes in the effective input capacitance C_x. Synchronous detection isolates signals of interest from unwanted signals [2].

Stray signals in the detection environment include alternating signal sources created by other fluorescent lamps, and other uncontrolled signal sources in the lamp and fixtures. An illustrative example considers the effect of low-frequency 1/f noise from the front-end op-amp as the unwanted signal on the output in the synchronous detection system. Figure 7 outlines the frequency domain treatment of the carrier and baseband signals in the presence of the stray signal which in this case is 1/f noise from the op-amp in the front-end amplifier.

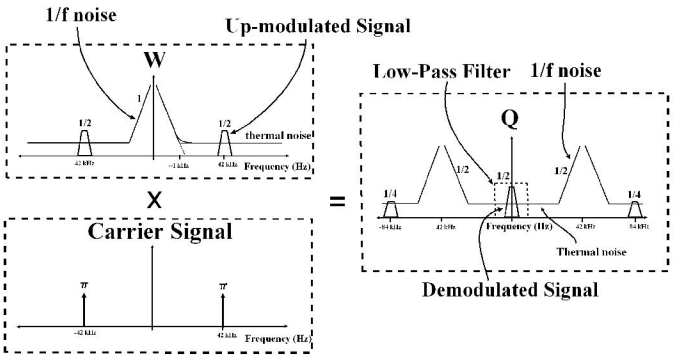

Fig. 7. Demodulation of the amplified up-modulated signal by multiplication with the carrier [2]

Due to the fact that amplification of the up-modulated signal takes place in the high frequency regime, the low-frequency or stray 1/f noise is left out of the final demodulated signal after low-pass filtering. Stray signals in the vicinity of the lamp sensor are treated like the 1/f noise from the amplifier; this example illustrates the specific advantage of using synchronous

detection in the context of rejecting low-frequency noise from the electronics that would otherwise be overwhelming. This principle is similar to chopper-stabilization of amplifiers for low-frequency signal amplification [2], [6]. A full schematic of the analog signal conditioning circuitry is shown in Figure 8. The topology remains differential until digitization and the multiplier is implemented as a fully-differential switching full-bridge multiplier.

III. Controlling the Sensing Range

The sensing range of the lamp sensor system can be controlled by utilizing the effect of the electrode configuration on the sensitivity of the differential measurement. In [1], the measured range test data showed that the sensitivity of the lamp decreased as the separation between the two electrodes (electrode spacing) decreased. This is intuitive because the difference measurement of the electric fields in front of the lamp should be smaller if the two electrodes are closer together. That is, as the length-scale of the separation of the electrodes decreases relative to the length-scale of the distance to the target, the differential measurement becomes weaker.

A. Multiple Electrode Pairs

In order to implement a lamp sensor which controls the sensing range by varying the electrode configuration, a prototype lamp sensor was built with multiple electrode pairs each at a different spacing. A photograph of the prototype lamp sensor with four electrode pairs is shown in Figure 9. In a practical lamp sensor, the electrodes in front of the lamp would be hidden as clear Indium Tin-Oxide electrodes implanted on the inside of the lamp cover [7]. A photograph of the electronics with four lamp sensor channels interfaced together for data analysis is shown in Figure 10.

Fig. 9. A photograph of the multiple electrode pair system setup [2]. In a practical lamp sensor, the electrodes in front of the lamp would be hidden as clear Indium Tin-Oxide electrodes implanted on the inside of the lamp cover [7].

A block diagram of the multiple channel system electronics is shown in Figure 11. For simplicity, relays disconnect the electrodes of unused channels from the inputs to their front-end amplifiers so that the unused electrodes are floating. A master PIC controls the four channels and an analog Multiplexer (MUX) for transmitting serial output data to a PC.

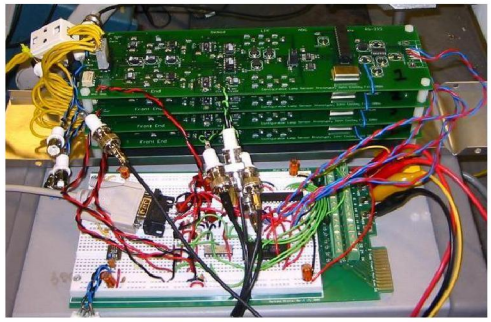

Fig. 10. A photograph of the multiple electrode pair system electronics [2]

B. Simulated Output

The dependence of the differential sensitivity on electrode spacing was simulated using FastCap and the calculated output from the capacitive circuit of Figure 3 [4]. The closed form expression of the differential output in response to varying capacitances in the capacitive circuit of Figure 3 can be found in [2]. In the simulation the human target, represented by a six-foot tall rectangular solid conductor, is always standing directly below one electrode in the hanging lamp sensor and the electrode spacing is varied symmetrically about the center of the lamp. The differential output voltage from the signal conditioning electronics is plotted in Figure 12. As expected, the simulation shows that the differential output voltage from the lamp sensor should increase for increasing electrode spacing.

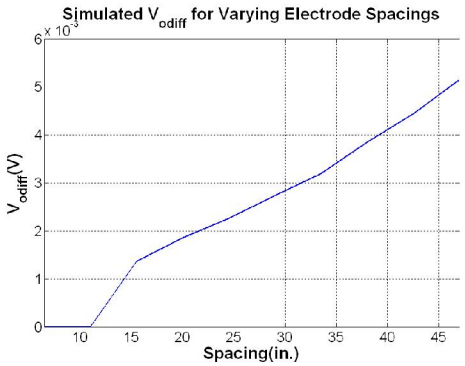

Fig. 12. A plot of the simulated output voltage for varying electrode spacings. The effective signal source strength is approximated as $1V_{rms}$ for the simulation as justified in [2].

C. Results and Data

An experiment was performed with the multiple electrode pair system. The goal of the experiment was to determine if the system could detect a change in the human target due to the possession or absence of a conducting (metallic) object.

Four different metallic objects were used. They were a large (30 lbs.) automotive alternator, a small (10 lbs.) automotive alternator, a large hollow metal box, and a small hollow metal box. The experiment was conducted as follows. The target walked below the lamp, stopping at one-foot intervals for each

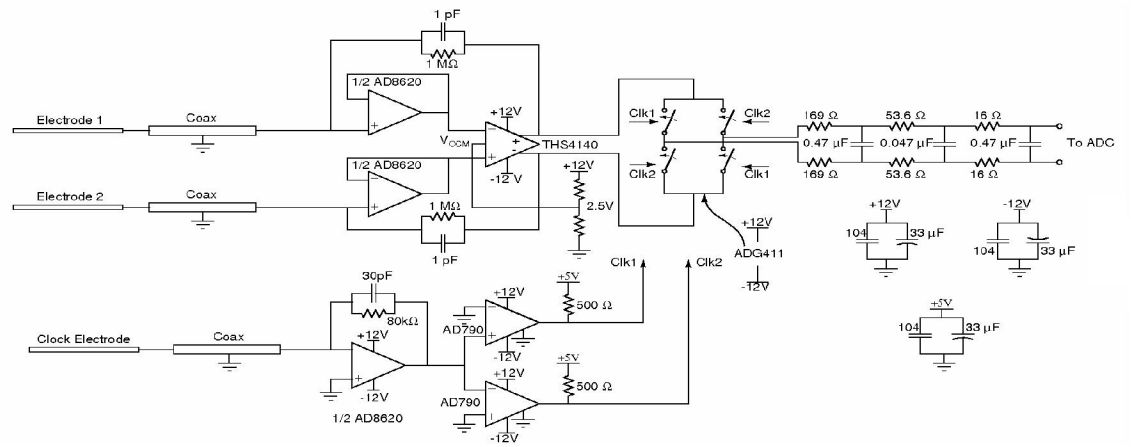

Fig. 8. The full schematic of the analog receiving network for the prototype lamp sensor channel [1], [2], [14]–[17]

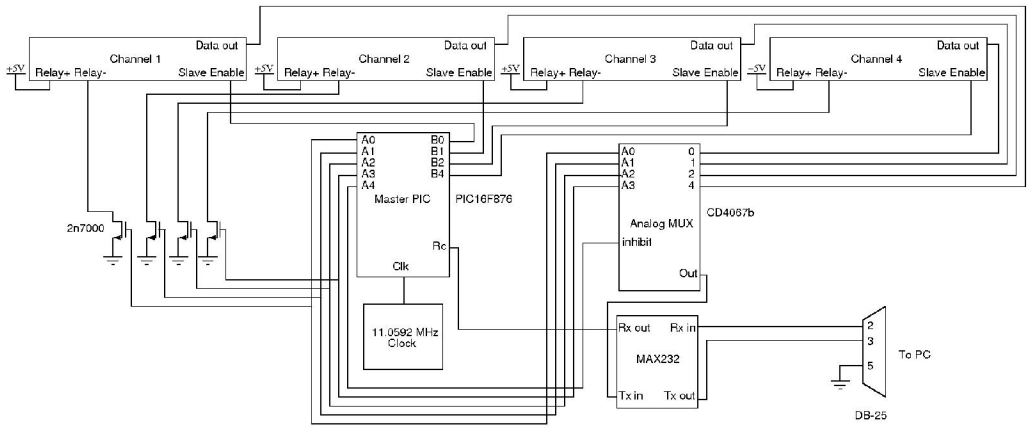

Fig. 11. The connection diagram for the prototype multiple channel system [2], [18]–[20]

polling of the electrode pairs. Each pass consisted of twelve one-foot steps each step corresponding to a measurement for all four electrode pairs. Each data set consisted of five complete passes. For reference, typical plots of measured and simulated output voltage from the lamp sensor for a passing human target are shown in Figures 13 and 14.

The metric for determining if the metallic object was detected was the rms ac output voltage of the passing sample for each channel. If the average rms ac output voltage of a data set consisting of five passes was different from the mean rms ac output voltage of the control data set with a confidence level of 97% or better, the data was considered a detection. To cross validate, a second control data set was taken after each data set and the first and second control data sets were also compared. The measured data set was only considered valid if the two control data sets were the same with a confidence level of at least 30%. This ensures that the difference between the first control data set and the measured data set was not a result of a slow and uncontrolled change in the output sensitivity of the system.

For each metallic object, data was taken while holding the object at waist, chest and then head levels. For each

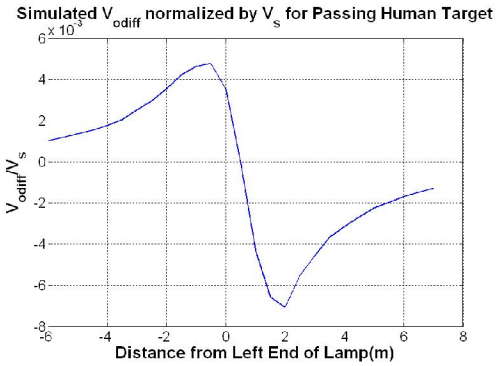

Fig. 13. An example plot the simulated output voltage as a human target passes below the lamp sensor [2]. The plot shown is simulated data for a human target passing at a range of 4ft. The output is normalized by the effective ac_{rms} source voltage V_s.

data set, the control set was taken with the human subject mimicking the body position that he would take on while holding the object. For instance, if the human subject would hold a metallic box at chest level, the control set was taken

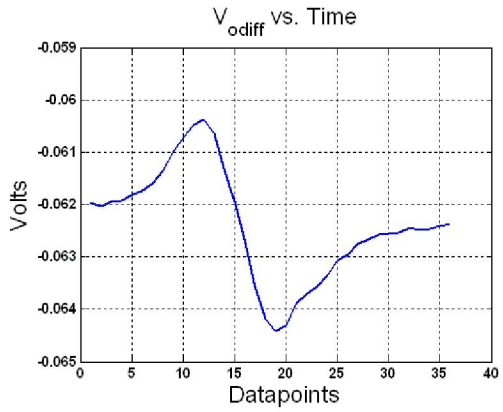

Fig. 14. An example plot of the measured output voltage as a human target passes below the lamp. The plot shown is data taken from a 6 ft. detection [2].

for the human passing under the lamp with arms bent as if holding a box at chest level. Therefore, control data sets were taken for each body position; for each object. The data was analyzed with a Z-test in MATLAB.

An overall control data set was taken comparing two data sets in which the human was carrying no metallic object. The overall control data is presented in Table II and shows no significant difference between the two data sets.

TABLE II
OVERALL CONTROL SAMPLE $p-values$ COMPARING TWO 10-SAMPLE CONTROL SETS FOR EACH CHANNEL WITH THE HUMAN TARGET CARRYING NO OBJECT.

Channel	Control
1	0.68
2	0.36
3	0.46
4	0.73

The detection data are presented in Table III. A low p-value means a low probability that the measured data set and the control data set were the same. Therefore, the lowest p-values represent the most confident detections. Data sets which correspond to detections based on the 97% detection rule are highlighted. In Table III, channel 1 is the widest-spaced electrode set corresponding to the longest detection range and channel 4 is the most closely-spaced electrode pair corresponding to the shortest detection range.

The data show clear detections for each of the metallic objects at some heights. Therefore, as a proof of concept, the lamp sensor system was shown to be potentially useful as a metal detector. Consistent with intuition, the larger the object and the closer to the lamp, the more likely it was to be detected on the human subject.

More interestingly, for some objects, only certain electrode configurations showed confident detections. For the small alternator, only the widest channels detected the object at waist and chest level. This follows the intuition that controlling the sensitivity of the lamp sensor can distinguish between different heights below the lamp. With the objects at the further ranges,

TABLE III
DETECTION DATA $p-values$ FOR VERTICAL SCANS OF A HUMAN WALKING BELOW THE LAMP HOLDING VARIOUS METALLIC OBJECTS [2]

Position/ Channel	Small Metal Box	Small Alternator	Large Metal Box	Large Alternator
head/1	3.01×10^{-23}	4.73×10^{-205}	8.60×10^{-22}	0
2	1.22×10^{-6}	2.80×10^{-17}	2.64×10^{-12}	2.30×10^{-129}
3	9.30×10^{-11}	3.22×10^{-10}	3.59×10^{-28}	5.70×10^{-130}
4	3.47×10^{-11}	2.32×10^{-44}	5.47×10^{-35}	0
chest/1	0.55	1.21×10^{-10}	1.31×10^{-7}	0.15
2	0.84	3.81×10^{-25}	9.78×10^{-5}	0.15
3	0.42	0.0013	0.0087	0.076
4	0.12	0.032	1.86×10^{-4}	0.027
waist/1	0.087	0.0010	0.88	4.55×10^{-5}
2	0.48	2.28×10^{-7}	0.35	1.93×10^{-12}
3	0.33	0.0032	0.57	3.41×10^{-10}
4	0.93	0.032	0.51	5.43×10^{-4}

only the electrode pairs with the highest sensitivities detected the object.

The large alternator data is also interesting. It shows that the vertical scanning may be selectively sensitive to certain objects at detection ranges bounding a range at which it is not detected or a range in which only one electrode pair detects the object. The data for the chest level large alternator was re-taken to confirm this. With each iteration, it showed the same result depicted in the table. Something particular to the large solid metallic object makes it less detectable at chest level in our experiments.

Potential applications of a vertically scanning, low-cost, discreet and widespread threat detector are numerous. Any public space or secure building in which security is a priority could make use of such a metal detector. The vertical scanning capability may also be a forerunner to a more complicated tomographic imaging functionality. By taking multiple independent measurements of the electric fields distorted by the presence of a conducting or dielectric object below the lamp, it may be possible to construct a dielectric tomographic surface which could reveal anomalies on the target corresponding to metallic objects or even dangerous substances. Such anomalies would be reported as anomalies in the three-dimensional space below the lamp so that the location of that object could be known with some precision. [2]

IV. LIMITATIONS AND FURTHER WORK

The lamp sensor with multiple electrode pairs demonstrated proof of concept for the ability to detect the difference between a human and the same human carrying a metallic object. This motivates further work in improving the system so that it can detect dielectric anomalies on a person without a priori knowledge of the response to the human target without the dielectric anomaly. Therefore, further work will improve the resolution and robustness of the lamp sensor and will investigate imaging techniques using multiple electrode measurements of the electric fields below the lamp to deduce the dielectric makeup of a target as it varies in the vertical axis.

The lamp sensor electronics have been designed so that they do not contribute significantly to the noise floor of the lamp

sensor system. The dominant noise source, and therefore the limiting factor in the resolution of the lamp sensor, is the signal source itself, i.e the bulbs and ballast. Therefore, improving the resolution of the lamp sensor requires an improvement in the noise content of the effective signal source. To achieve this, we are pursuing differential-mode feedforward compensation to actively cancel the signal source noise. Similar techniques are discussed in [8]–[11]. The implementation of feedforward compensation in the modulation scheme would require a division to eliminate intensity noise since it appears as random modulations of the carrier signal. Low-noise, high-frequency analog division may be achieved with current-mode translinear circuits. Examples of translinear design with current-mode circuits for synthesis of analog dividers can be found in [12], [13].

Finally, before approaching the problem of actively canceling signal source noise with feedforward compensation, a better understanding of the origin of the alternating surface potential of the bulb is required as it pertains to the alternation of the lengthwise potential distribution. Also, a quantitative analysis of random signal source modulations both differential-mode (localized along the length of a bulb) and common-mode will be required.

V. Conclusion

In conclusion, the lamp sensor system achieves good sensitivity to the presence and motion of human targets below the lamp by employing various circuit and signal processing techniques. These techniques include differential measurement, current-mode detection, and synchronous detection. Furthermore, the lamp sensor demonstrated proof of concept for detecting the change in the dielectric makeup of a human target with and without metallic objects. In order for the system to be used as a robust metal or dangerous substance detector, the signal source must be made less sensitive to noise and more predictable. Then, techniques for deducing the variation in dielectric makeup of a target as it varies along the vertical axis must be implemented in order to detect the presence of a dielectric anomaly on the target without a-priori knowledge of the targets dielectric makeup.

Acknowledgment

We would like to acknowledge the generous support for this research by the United States Department of Justice and the Grainger Foundation.

References

[1] John Cooley, Al-Thaddeus Avestruz, and Steven B. Leeb, "Proximity Detection and Ranging Using a Modified Fluorescent Lamp for Security Applications." Proceedings of the IEEE International Carnahan Conference on Security Technology 2006 (ICCST06).

[2] John J. Cooley, *Capacitive Sensing with a Fluorescent Lamp*, MIT Master of Engineering Theses, 2007.

[3] James K. Roberge. *Operational Amplifiers: Theory and Practice John Wiley and Sons, Inc., New York, London, Sydney, Toronto, 1975.*

[4] K. Nabors, et al. "Multipole-accelerated capacitance extraction algorithms for 3-D structures with muliple dielectrics." *IEEE Transactions Circuits and Sytems-I: Fundamental Theory and Applications, vol. 39, pp. 946-954, Nov. 1992.*

[5] James T. Dakin. "Nonequilibrium Lighting Plasmas". *IEEE Transactions on Plasma Science*, Vol. 19, No. 6, 1991.

[6] Christian C. Enz, Gabor C. Temez. "Circuit Techniques for Reducing the Effects of Op-Amp Imperfections: Autozeroing, Correlated Double Sampling, and Chopper Stabilization." *Proceedings of the IEEE, Vol. 84, No. 11, November 1996.*

[7] C. L. Chua, R.L. Thornton, D.W. Treat, V.K. Yang, and C. C. Dunnrowicz. "Indium Tin Oxide Transparent Electrodes for Broad-Area Top-Emitting Vertical-Cavity Lasers". *IEEE Photonics Technology Letters*, Vol. 9, No. 5, 1997.

[8] Lap-Shun Fock, Anthony Kwan, and Rodney S. Tucker. "Reduction of Semiconductor Laser Intensity Noise by Feedforward Compensation: Experiment and Theory" *Journal of Lightwave Technology, Vol. 10, No. 12, December 1992.*

[9] L. S. Fock, R. S. Tucker. "Simultaneous Reduction of Intensity Noise and Distortion in Semiconductor Lasers by Feedforward Compensation." *Electronics Letters 4th July 1991 Vol. 27 No. 14.*

[10] Adrian J. Keating and David D. Sampson. "Reduction of Excess Intensity Noise in Spectrum-Sliced Incoherent Light for WDM Applications." *Journal of Lightwave Technology, Vol. 10, No. 12, December 1992.*

[11] Jie Zeng and R. A. de Callafon. "Feedforward estimation for active noise cancellation in the presence of acoustic coupling." *43rd IEEE Conference on Decision and Control, December 14-17, 2004, Atlantis, Paradise Island, Bahamas.*

[12] Weixin Gai, Hongyi Chen and E. Seevinck. "Quadratic-translinear CMOS multiplier-divider circuit." *Electronics Letters 8th May 1997 Vol. 33 No. 10.*

[13] Edgar Sánchez-Sinencio, Jaime Ramírez-Angulo, Bernabé Linares-Barranco, and Angel Rodríguez-Vázquez. "Operational Transconductance Amplifier-Based Nonlinear Function Syntheses." *IEEE Journal of Solid-State Circuits, Vol. 24, No. 6, December 1989.*

[14] "AD8610 data sheet". Analog Devices. Norwood, MA, USA.

[15] "THS4140 data sheet." Texas Instruments. Dallas, TX, USA.

[16] "AD790 data sheet." Analog Devices. Norwood, MA, USA.

[17] "ADG411 data sheet." Analog Devices. Norwood, MA, USA.

[18] "PIC16F876 data sheet." Microchip Technology Corp. USA

[19] "CD4067b data sheet." Texas Instruments. Dallas, TX, USA.

[20] "ECS-100 Oscillator data sheet." ECS Inc. Olathe, KS, USA.

VI. Vitae

John Cooley is currently a Ph.D. candidate at the Massachusetts Institute of Technology studying Electrical Engineering. He received the S.B. degree in Electrical Engineering and the S.B. degree in Physics in 2005 at MIT, and the Master of Engineering degree in Electrical Engineering in 2007 at MIT. His research interests include electrodynamics, capacitive sensors, and low-noise analog electronics design.

Al-Thaddeus Avestruz is currently a Ph.D candidate in Electrical Engineering at the Massachusetts Institute of Technology. He received his S.B. in Physics in 1994 and his S.M. and Engineer's degrees in 2006, also at MIT. He has worked for a number of companies including Teradyne Corporation, Diversified Technologies and Talking lights, LLC. His research interests include circuit design, sensors, electro-magnetics and electrical machinery, embedded systems, alternative energy and power electronics.

Dr. Steven B. Leeb received S.B., S.M., E.E. and Ph.D. degrees from MIT. He has been a member of the MIT faculty in the Department of Electrical Engineering and Computer Science since 1993. He serves as a professor in the Laboratory for Electromagnetic and Electronic Systems. He is concerned with the design, development, maintenance, and security processes for all kinds of machinery with electrical actuators, sensors, or power electronic drives.